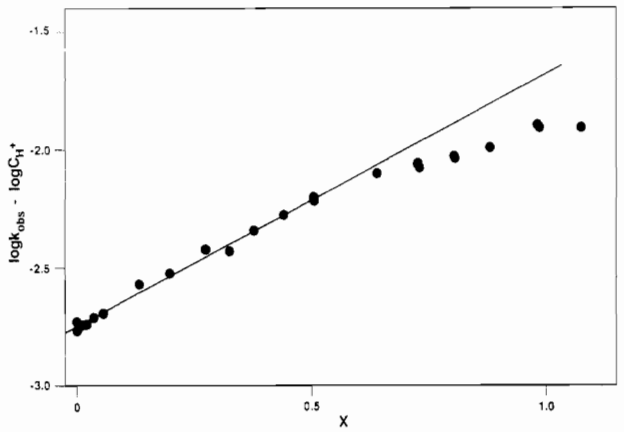

Figure 3. Plot of log k_{obsd} − log C_{H^+} vs. X (eq 8) for ligand dissociation from $CF_3Co(D_2H_2)MeIm$. The solid line is a least-squares fit to the data between $X = 0.0013$ and $X = 0.639$, with slope 1.07 ± 0.03, intercept −2.75 ± 0.01, and $r^2 = 0.992$.

value considering the fact that pK_2^{py} is −1.65 and 1-methylimidazole ($pK_a = 7.29$) is nearly 2 orders of magnitude more basic than pyridine ($pK_a = 5.51$[19]). In addition, if this interpretation (i.e., Scheme II) is correct, the region of the H–rate profile up to the inflection (i.e., $H >$ ca −0.75) would be governed by the simple rate law of eq 6. It is consequently possible to use the

$$k_{obsd} = k_{off} + k_{H^+}a_{H^+} \quad (6)$$

Cox and Yates generalized acidity function (eq 1) to determine what acidity function (i.e., what value of m^*) is appropriate for k_{H^+}. Expressing hydrogen ion activity via this acidity function leads to the rate law of eq 7, and for all acidities at which $k_{off} \ll k_{H^+}a_{H^+}$ eq 8 will hold. Hence, a plot of log k_{obsd} − log C_{H^+} vs.

$$k_{obsd} = k_{off} + k_{H^+}10^{m^*X+\log C_{H^+}} \quad (7)$$

$$\log k_{obsd} = \log k_{H^+} + m^*X + \log C_{H^+} \quad (8)$$

X should be linear with slope m^* and intercept log k_{H^+}. Such a plot is shown in Figure 3 and can be seen to be satisfactorily linear between $X = 0.0013$ ($H = 1.94$ at $m^* = 0.77$) and $X = 0.639$ ($H = -0.80$ at $m^* = 0.77$). At higher acidities the plot curves downward, confirming the downward inflection in the H–rate profile at $H < -0.75$. From the linear portion of the plot $k_{H^+} = 1.77 \times 10^{-3}$ M^{-1} s^{-1} and $m^* = 1.07 \pm 0.03$. Disappointingly, attempts to titrate the lower protonation of MeIm spectrophotometrically in order to determine the appropriate acidity function (i.e., m^* value) and hence to see if k_{H^+} follows the same acidity function as N-1 protonation of cationic $MeImH^+$ were unsuccessful due to the negligibly small spectral changes accompanying N-1 protonation of the $MeImH^+$ cation. However, the protonation of many nitrogen weak bases has been studied. The substituted-aniline indicator system originally used by Hammett and Dyrup to establish the H_0 acidity function and related compounds usually regarded as Hammett indicators follows the generalized acidity function with $m^* = 1.02 \pm 0.08$.[54] In addition, one of us and others[48] previously found the spectral changes accompanying N-1 protonation of α-ribazole (1-α-D-ribofuranosyl-5,6-dimethylbenzimidazole) to follow the H_0 acidity function. It thus seems reasonable to suggest that the kinetics of MeIm dissociation follow the Hammett acidity function, H_0, and that MeIm dissociation from $CF_3Co(D_2H_2)MeIm$ is indeed subject to specific-acid catalysis via protonation at N-1. However, given the limitations of the data collectible for this system, this must be considered to remain an open question until an appropriate experimental system can be devised to provide a definitive answer.

Acknowledgment. This research was supported by the Robert A. Welch Foundation, Houston, TX (Grant No. Y-749).

Contribution from the Departments of Chemistry, Wayne State University, Detroit, Michigan 48202, and University of Wisconsin at Eau Claire, Eau Claire, Wisconsin 54701

Structure–Reactivity Relationships in Copper(II)/Copper(I) Electron-Transfer Kinetics: Evaluation of Self-Exchange Rate Constants for Copper–Polythia Ether Complexes

Michael J. Martin,[1a] John F. Endicott,[1a] L. A. Ochrymowycz,[1b] and D. B. Rorabacher*[1a]

Received June 25, 1986

Kinetic parameters are reported for electron-transfer cross-reactions of eight Cu(II)/Cu(I) systems involving closely related open-chain and macrocyclic polythia ether ligands. Both the oxidation kinetics of the Cu(I) species and the reduction kinetics of the Cu(II) species are included by using tris(4,7-dimethyl-1,10-phenanthroline)iron(III) and diaquo(2,3,9,10-tetramethyl-1,4,8,11-tetraazacyclotetradeca-1,3,8,10-tetraene)cobalt(II) as the principal cross-reagents. Reactions with other cross-reagents are also reported for selected Cu(II)/Cu(I) systems. The applicability of the Marcus cross-relation to these reactions is examined and is shown to yield calculated Cu(II)/Cu(I) self-exchange rate constants that differ significantly for the corresponding oxidation and reduction reactions. To account for these apparent discrepancies, a dual-pathway mechanism is proposed in which a major part of the conformational reorganization at the copper center occurs sequentially, rather than concertedly, with the electron-transfer step. Differences in the relative kinetic behavior of the various copper–polythia ether complexes are discussed in terms of the influence of ligand constraints upon the bond-making and bond-breaking sequences that accompany the conversion of Cu(II) to Cu(I) (and vice versa).

Introduction

The prevalence of the Cu(II)/Cu(I) redox couple in enzymes involved in biological oxidation–reduction processes[2,3] has stimulated a high level of interest in the mechanistic details associated with electron transfer at a copper center. Specific attention has been focused on the kinetics of the blue electron carriers (azurin, plastocyanin, rusticyanin, stellacyanin), which contain a single copper atom and appear to exhibit relatively large self-exchange rate constants (eq 1) on the order of $k_{11} = 10^4$–10^6 M^{-1} s^{-1}.[4-19]

$$*Cu^{II} + Cu^{I} \underset{}{\overset{k_{11}}{\rightleftharpoons}} *Cu^{I} + Cu^{II} \quad (1)$$

(1) (a) Wayne State University. (b) University of Wisconsin at Eau Claire.
(2) *Copper Coordination Chemistry: Biochemical and Inorganic Perspectives*; Karlin, K. D., Zubieta, J., Eds.; Adenine: Guilderland, NY, 1983.
(3) (a) *Met. Ions Biol. Syst.* **1981**, *13*. (b) Owen, C. A., Jr. *Biological Aspects of Copper*; Noyes: Park Ridge, NJ, 1982. (c) *Copper Proteins and Copper Enzymes*; Lontie, R., Ed.; CRC: Boca Raton, FL, 1984; Vols. I–III.
(4) (a) Holwerda, R. A.; Wherland, S.; Gray, H. B. *Annu. Rev. Biophys. Bioeng.* **1976**, *5*, 363–396 and references therein. (b) Cummins, D.; Gray, H. B. *J. Am. Chem. Soc.* **1977**, *99*, 5158–5167. (c) Holwerda, R. A.; Knaff, D. B.; Gray, H. B.; Clemmer, J. D.; Crowley, R. A.; Smith, J. M.; Mauk, A. G. *Ibid.* **1980**, *102*, 1142–1146.
(5) Farver, O.; Pecht, I. In *Copper Proteins*; Spiro, T. G., Ed.; Wiley-Interscience: New York, 1981; pp 151–192 and references therein.

0020-1669/87/1326-3012$01.50/0 © 1987 American Chemical Society

Crystal structures of oxidized azurin and plastocyanin have revealed that the copper in these proteins is constrained by the protein matrix to adopt a distorted tetrahedral coordination geometry.[20-22] This geometry is presumed to undergo little change upon reduction of the copper center.[23] In conjunction with the hydrophobic environment of the copper atom (thereby minimizing or eliminating solvent reorganization contributions), this relatively rigid geometry should result in a small Franck–Condon barrier for reaction 1, thereby accounting for the observed rapid electron exchange.[24]

For electron-transfer reactions involving unconstrained low molecular weight copper complexes, a much larger Franck–Condon barrier is anticipated[24] in view of the large changes brought about in the inner-coordination sphere of the copper atom upon converting from 6-coordinate (tetragonal) or 5-coordinate (square-pyramidal or trigonal-bipyramidal) Cu(II) to 4-coordinate (tetrahedral) Cu(I).[25] Thus, it is commonly believed that the utilization of sterically hindered or rigid chelating ligands or other constrained environments might result in a significant lowering of the Franck-Condon barrier, which would then be reflected in an increased value for the Cu(II)/Cu(I) self-exchange rate constant.[24] Attempts to demonstrate this behavior have been largely unsuccessful, however.[26,27]

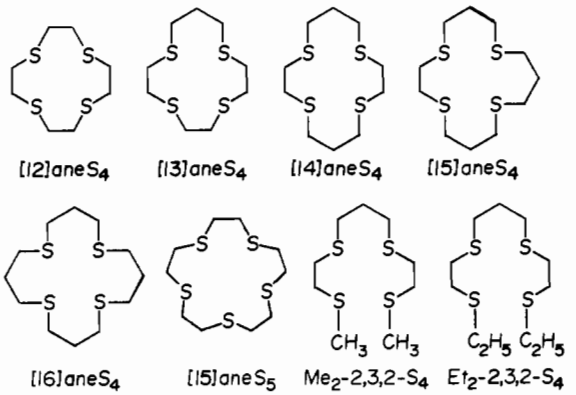

Figure 1. Ligands included in this work.

Most electron-transfer kinetic studies on low molecular weight copper complexes have involved the *reduction* of the Cu(II) species by using agents that are known (or presumed) to promote outer-sphere electron-transfer pathways (eq 2).[28-32] The Marcus

$$Cu^{II}L + A_{Red} \xrightarrow{k_{12}} Cu^{I}L + A_{Ox} \qquad (2)$$

cross-relation[33] has then been applied to the experimental k_{12} values to estimate the Cu(II)/Cu(I) self-exchange rate constant, k_{11}. With few exceptions, the k_{11} values calculated in this manner are considerably smaller than the k_{11} values obtained for the copper proteins, an observation that has been attributed to the larger Franck–Condon barriers. However, for the few instances in which kinetic studies have been made on the *oxidation* of corresponding Cu(I) species (eq 3), the calculated k_{11} values have been as large

$$Cu^{I}L + B_{Ox} \xrightarrow{k_{31}} Cu^{II}L + B_{Red} \qquad (3)$$

as, or larger than, those reported for the copper proteins.[34]

Lee and Anson[35] have suggested that the apparent discrepancy in k_{11} values calculated from the two types of cross-reactions may be inherent in copper systems as a result of unequal reorganization energies for Cu(II) and Cu(I). Thus, a more representative self-exchange rate constant for Cu(II)/Cu(I) systems may be obtained by combining the reorganizational energies evaluated from reactions 2 and 3. In a subsequent test of this hypothesis,[36] these workers obtained a direct estimate of the self-exchange rate constant for $Cu(phen)_2^{2+/+}$ (phen = 1,10-phenanthroline) from a voltammetric study, the resulting value ($k_{11} \sim 10^5$ M^{-1} s^{-1}) being essentially the geometric mean of the k_{11} values calculated independently by means of reactions 2 and 3 ($k_{11} = 50$ M^{-1} s^{-1} [26] and 5×10^7 M^{-1} s^{-1},[34] respectively).

(6) Sykes, A. G. *Chem. Soc. Rev.* **1985**, *14*, 283–315.
(7) (a) Segal, M. G.; Sykes, A. G. *J. Am. Chem. Soc.* **1978**, *100*, 4585–4592. (b) Lappin, A. G.; Segal, M. G.; Weatherburn, D. C.; Sykes, A. G. *Ibid.* **1979**, *101*, 2297–2301. (c) Lappin, A. G.; Segal, M. G.; Weatherburn, D. C.; Henderson, R. A.; Sykes, A. G. *Ibid.* **1979**, *101*, 2302–2306. (d) Sisley, M. J.; Segal, M. G.; Stanley, C. S.; Adzamli, I. K.; Sykes, A. G. *Ibid.* **1983**, *105*, 225–228. (e) Chapman, S. K.; Sanemasa, I.; Watson, A. D.; Sykes, A. G. *J. Chem. Soc., Dalton Trans*, **1983**, 1949–1953. (f) Chapman, S. J.; Watson, A. D.; Sykes, A. G. *Ibid.* **1983**, 2543–2548. (g) Chapman, S. K. Sanemasa, I.; Sykes, A. G. *Ibid.* **1983**, 2549–2553. (h) Augustin, M. A.; Chapman, S. K.; Davies, D. M.; Watson, A. D.; Sykes, A. G. *J. Inorg. Biochem.* **1984**, *20*, 281–289. (i) Chapman, S. K.; Knox, C. V.; Kathirgamanathan, P.; Sykes, A. G. *J. Chem. Soc., Dalton Trans.* **1984**, 2769–2773. (j) Chapman, S. K.; Knox, C. V.; Sykes, A. G. *Ibid.* **1984**, 2775–2780.
(8) Augustin, M. A.; Chapman, S. K.; Davies, D. M.; Sykes, A. G.; Speck, S. H.; Margoliash, E. *J. Biol. Chem.* **1983**, *258*, 6405–6409.
(9) McArdle, J. V.; Coyle, C. L.; Gray, H. B.; Yoneda, G. S.; Holwerda, R. A. *J. Am. Chem. Soc.* **1977**, *99*, 2483–2489.
(10) Antonini, E.; Finazzi-Agro, A.; Avigliano, L.; Guerrieri, P.; Rotilla, G.; Mondovi, B. *J. Biol. Chem.* **1970**, *245*, 4847–4849.
(11) Silvestrini, M. C.; Brunori, M.; Wilson, M. T.; Darley-Usmar, V. M. *J. Inorg. Biochem.* **1981**, *14*, 327–338.
(12) Canters, G. W.; Hill, H. A. O.; Kitchen, N. A.; Adman, E. T. *J. Magn. Reson.* **1984**, *57*, 1–23.
(13) Cho, K. C.; Austin, R. H. *J. Chem. Phys.* **1984**, *80*, 1131–1134.
(14) Takenaka, K.; Takabe, T. *J. Biochem.* **1984**, *96*, 1813–1824.
(15) King, G. C.; Binstead, R. A.; Wright, P. E. *Biochim. Biophys. Acta* **1985**, *806*, 262–271.
(16) Bottin, H.; Mathis, P. *Biochemistry* **1985**, *24*, 6453–6460.
(17) Armstrong, F. A.; Driscoll, P. C.; Hill, H. A. O. *FEBS Lett.* **1985**, *190*, 242–248.
(18) Pladziewicz, J. R.; Brenner, M. S.; Rodenberg, D. A.; Likar, M. D. *Inorg. Chem.* **1985**, *24*, 1450–1453.
(19) Lappin, A. G.; Lewis, C. A.; Ingledew, W. J. *Inorg. Chem.* **1985**, *24*, 1446–1450.
(20) (a) Colman, P. M.; Freeman, H. C.; Guss, J. M.; Murata, M.; Norris, V. A.; Ramshaw, J. A. M.; Venkatappa, M. P. *Nature (London)* **1978**, *272*, 319–324. (b) Guss, J. M.; Freeman, H. C. *J. Mol. Biol.* **1983**, *169*, 521–563.
(21) Adman, E. T.; Stenkamp, R. E.; Sieker, L. C.; Jensen, L. H. *J. Mol. Biol.* **1978**, *123*, 35–47.
(22) Norris, G. E.; Anderson, B. F.; Baker, E. N. *J. Mol. Biol.* **1983**, *165*, 501–521.
(23) Freeman, H. C. In *Coordination Chemistry*; Laurent, J. P., Ed.; Pergamon: Oxford, England, 1981; Vol. 21, pp 29–51.
(24) (a) Williams, R. J. P. *Inorg. Chim. Acta Rev.* **1971**, *5*, 137–155. (b) Vallee, B. L.; Williams, R. J. P. *Proc. Natl. Acad. Sci. U.S.A.* **1968**, *59*, 498–505.
(25) (a) Hathaway, B. J. *Coord. Chem. Rev.* **1981**, *35*, 211–252. (b) Hathaway, B. J.; Billing, D. E. *Ibid.* **1970**, *5*, 143–207.
(26) Karlin, K. D.; Yandell, J. K. *Inorg. Chem.* **1984**, *23*, 1184–1188.
(27) Lappin, A. G.; Peacock, R. D. *Inorg. Chim. Acta* **1980**, *46*, L71–L72.
(28) (a) Yandell, J. K. In *Copper Coordination Chemistry: Biochemical and Inorganic Perspectives*; Karlin, K. D., Zubieta, J., Eds.; Adenine: Guilderland, NY, 1983; pp 157–166 and references therein. (b) Augustin, M. A.; Yandell, J. K. *Inorg. Chim. Acta* **1979**, *37*, 11–18. (c) Augustin, M. A.; Yandell, J. K. *Inorg. Chem.* **1979**, *18*, 577–583. (d) Augustin, M. A.; Yandell, J. K.; Addison, A. W.; Karlin, K. D. *Inorg. Chem. Acta* **1981**, *55*, L35–L37.
(29) Aoi, N.; Matsubayashi, G.; Tanaka, T. *J. Chem. Soc., Dalton Trans.* **1983**, 1059–1066.
(30) (a) Al-Shatti, N.; Lappin, A. G.; Sykes, A. G. *Inorg. Chem.* **1981**, *20*, 1466–1469. (b) Leupin, P.; Al-Shatti, N.; Sykes, A. G. *J. Chem. Soc., Dalton Trans.* **1982**, 927–930.
(31) Davies, K. M. *Inorg. Chem.* **1983**, *22*, 615–619.
(32) (a) Clemmer, J. D.; Hogaboom, G. K.; Holwerda, R. A. *Inorg. Chem.* **1979**, *18*, 2567–2572. (b) Holwerda, R. A. *Ibid.* **1982**, *21*, 2107–2109.
(33) (a) Marcus, R. A. *J. Chem. Phys.* **1956**, *24*, 966–978. (b) Marcus, R. A. *Discuss. Faraday Soc.* **1960**, *29*, 21–31. (c) Marcus, R. A. *J. Chem. Phys.* **1965**, *43*, 679–701. (d) Marcus, R. A.; Sutin, N. *Biochim. Biophys. Acta* **1985**, *811*, 265–322.
(34) Yoneda, G. S.; Blackmer, G. L.; Holwerda, R. A. *Inorg. Chem.* **1977**, *16*, 3376–3378. Cf.: deAraujo, M. A.; Hodges, H. L. *Ibid.* **1982**, *21*, 3167–3172.
(35) Lee, C. W.; Anson, F. C. *J. Phys. Chem.* **1983**, *87*, 3360–3362.
(36) Lee, C. W.; Anson, F. C. *Inorg. Chem.* **1984**, *23*, 837–844.

Pulliam and McMillan[37] used NMR line-broadening techniques to obtain a direct determination of the self-exchange rate constant for a rigid planar copper complex. This approach should also yield a combination of the reorganizational energies contributed by Cu(II) and Cu(I). Despite the geometric constraints inherent in their system, however, the resolved k_{11} value (5×10^5 M^{-1} s^{-1}) differed little from Lee and Anson's value for $Cu(phen)_2^{2+/+}$.

The cumulated kinetic studies on electron-transfer reactions involving low molecular weight copper complexes that have been reported to date have failed to establish a direct correlation between the magnitude of resolved self-exchange rate constants and the extent to which the inner-coordination sphere is constrained. Part of this difficulty may revolve around the degree to which the Marcus theory is applicable to systems in which there is bond making or bond breaking.

On the basis of Lee and Anson's hypothesis, it would appear that any effort to obtain representative self-exchange rate constants of Cu(II)/Cu(I) systems must involve the study of both the oxidation of the Cu(I) species and the reduction of the corresponding Cu(II) species, either directly via reaction 1 or independently via reactions 2 and 3. In the current investigation, we have taken the latter approach to determine apparent self-exchange rate constants for a closely related series of copper–polythia ether complexes. The crystal structures of all of the Cu(II) complexes[38-40] and some of the Cu(I) complexes[39,40] have already been determined, thereby providing relevant information on the structural changes presumed to accompany electron transfer at the copper center. These results provide the first comparative study on the relative self-exchange rate constants of a homologous series of copper complexes in which the potential reorganization problems proposed by Lee and Anson have been considered.

The specific systems for which kinetic data are reported in this work include the copper complexes of the following eight macrocyclic and open-chain polythia ethers: 1,4,7,10-tetrathiacyclododecane ([12]aneS$_4$); 1,4,7,10-tetrathiacyclotridecane ([13]aneS$_4$); 1,4,8,11-tetrathiacyclotetradecane ([14]aneS$_4$); 1,4,8,12-tetrathiacyclopentadecane ([15]aneS$_4$); 1,5,9,13-tetrathiacyclohexadecane ([16]aneS$_4$); 1,4,7,10,13-pentathiacyclopentadecane ([15]aneS$_5$); 2,5,9,12-tetrathiatridecane (Me$_2$-2,3,2-S$_4$); and 3,6,10,13-tetrathiapentadecane (Et$_2$-2,3,2-S$_4$). All eight ligands (see Figure 1) form stable Cu(I) complexes, thereby circumventing one of the difficulties that has tended to plague oxidation studies on many other low molecular weight copper systems. Since these complexes are also unaffected by changes in acidity, it has been possible to conduct all studies in pH regions that are optimal for the cross-reaction reagents.

Experimental Section

Reagents. Preparation and purification of $Cu(ClO_4)_2 \cdot 6H_2O$ and the several polythia ether ligands have been previously described.[41] Literature methods were used for the synthesis and purification of the several electron-transfer reagents utilized including $Na_3IrCl_6 \cdot 2H_2O$,[42] diaquo(2,3,9,10-tetramethyl-1,4,8,11-tetraazacyclotetradeca-1,3,8,10-tetraene)cobalt(II) perchlorate (i.e., $[Co^{II}(Me_4[14]tetraeneN_4)(H_2O)_2](ClO_4)_2$),[43] tris(4,7-dimethyl-1,10-phenanthroline)iron(III) perchlorate trihydrate (i.e., $[Fe^{III}(4,7\text{-}Me_2phen)_3](ClO_4)_3 \cdot 3H_2O$),[44] and tetraammine(bipyridyl)ruthenium(II) perchlorate (i.e., $[Ru^{II}(NH_3)_4(bpy)](ClO_4)_2$).[45]

Table I. Approximate Formal Electrode Potentials for Copper(II)/Copper(I)–Polythia Ether Systems As Estimated from Slow-Scan Cyclic Voltammetry and from Homogeneous Oxidation and Reduction Cross-Reaction Kinetics, in Aqueous Solution at 25 °C, μ = 0.10 M

complexed ligand	$E_{1/2}$,[a] V	E_{11}^f(comb),[b] V
[12]aneS$_4$	0.641	0.853, 0.860
[13]aneS$_4$	0.595	0.842
[14]aneS$_4$	0.600	0.695, 0.707
[15]aneS$_4$	0.630[c]	0.715
[16]aneS$_4$	0.685[c]	0.793
Me$_2$-2,3,2-S$_4$	0.818	1.030
Et$_2$-2,3,2-S$_4$	(0.818)[d]	1.023
[15]aneS$_5$	0.752	0.778, 0.777

[a] $E_{1/2} = (E_a + E_c)/2$ vs. NHE as determined from slow-scan cyclic voltammetry.[46] [b] E_{11}^f(comb) values (vs. NHE) were calculated from eq 20 by using K_{12} or K_{31} values computed from the substitution of k_{11}(comb) (eq 28) into eq 18 or eq 19 (see text). [c] Revised values recently obtained in this laboratory from new slow-scan cyclic voltammetric and controlled-potential electrolysis measurements.[59] [d] Value assumed equal to $E_{1/2}$ for $Cu(Me_2\text{-}2,3,2\text{-}S_4)^{2+/+}$ by analogy to corresponding behavior in 80% methanol.[46]

Pure $NaClO_4$ was prepared by slowly adding reagent grade NaOH pellets to relatively concentrated $HClO_4$ (reagent grade, G. F. Smith Chemical Co.) and evaporating to yield colorless crystals, which were recrystallized once from water. Impure CF_3SO_3H (Alpha Products or 3M Co.) was distilled twice at atmospheric pressure in an all smooth glass apparatus (using a nitrogen bubbler to prevent bumping) to yield a colorless liquid, which was then stored in a glass bottle with a Teflon-lined cap. Deionized–distilled water of conductivity grade was used in the preparation of all solutions.

Copper(II)–polythia ether solutions were prepared by dissolving a weighed portion of the appropriate polythia ether ligand in a standard $Cu(NO_3)_2$ or $Cu(ClO_4)_2$ solution, filtering off any undissolved ligand, and titrating potentiometrically against standard $Hg(ClO_4)_2$ (prepared from reagent grade HgO and $HClO_4$) to determine the total ligand concentration in solution. (Note: If a Hg pool indicating electrode is used, sharper end points are achieved if the Cu–polythia ether solution is used as the titrant.) Copper(I)–polythia ether solutions were prepared by constant-potential electrolysis under an atmosphere of scrubbed nitrogen. Stock solutions of Na_3IrCl_6, $Ru^{II}(NH_3)_4$bpy, and $Co^{II}(Me_4[14]tetraeneN_4)$ were prepared by dissolving weighed amounts of the corresponding salts in deaerated 0.10 M $HClO_4$, solutions of the former two reagents being protected from light. Stock solutions of $Fe^{III}(4,7\text{-}Me_2phen)_3$ were prepared by dissolving weighed amounts of the perchlorate salt in deaerated 0.10 M CF_3SO_3H.

Instrumentation. All absorbance spectra were obtained on a Cary Model 17D dual-beam recording spectrophotometer. For reactions involving $IrCl_6^{2-}$ as reagent, a Xenon Corp. Model A flash photolysis system was utilized. The quartz sample cell, with an inner path length of 20 cm, was fitted with a deaeration device and was surrounded by an outer jacket to provide for the use of a liquid filter, which was then circulated through a temperature bath to thermostat the sample solution. All other kinetic measurements were made with a thermostated Durrum Model D-110 stopped-flow spectrophotometer equipped with glass and Kel-F tubings and fittings and gastight syringes. For measurements conducted at 5.5 and 15.0 °C, the actual temperature within the reaction cell was determined by removing the stopping syringe and the No. 5 (flushing) valve block and inserting a calibrated precision thermistor probe (No. 44105, Yellow Springs Instruments) through the exit channel into the observation chamber. The kinetic absorbance curves were recorded and evaluated as previously described.[41] For slower reactions ($t_{1/2}$ > 10 s), a Hewlett-Packard Model 7047-A X-Y plotter was used to record the data.

For electrochemical measurements, a Princeton Applied Research system was employed consisting of a Model 175 universal programmer (to control potentials), a Model 173 potentiostat–galvanostat (to measure currents), and a Model 178 electrometer (to minimize electrical noise).

Results

Potential Measurements. Approximate formal potential values for all $CuL^{2+/+}$ systems included in this study were estimated from

(37) Pulliam, E. J.; McMillan, D. R. *Inorg. Chem.* **1984**, *23*, 1172–1175.
(38) Pett, V. B.; Diaddario, L. L., Jr.; Dockal, E. R.; Corfield, P. W. R.; Ceccarelli, C.; Glick, M. D.; Ochrymowycz, L. A.; Rorabacher, D. B.; *Inorg. Chem.* **1983**, *22*, 3661–3670.
(39) Diaddario, L. L., Jr.; Dockal, E. R.; Glick, M. D.; Ochrymowycz, L. A.; Rorabacher, D. B. *Inorg. Chem.* **1985**, *24*, 356–363.
(40) Corfield, P. W. R.; Ceccarelli, C.; Glick, M. D.; Moy, I. W.-Y.; Ochrymowycz, L. A.; Rorabacher, D. B. *J. Am. Chem. Soc.* **1985**, *107*, 2399–2404.
(41) Diaddario, L. L.; Zimmer, L. L.; Jones, T. E.; Sokol, L. S. W. L.; Cruz, R. B.; Yee, E. L.; Ochrymowycz, L. A.; Rorabacher, D. B. *J. Am. Chem. Soc.* **1979**, *101*, 3511–3520.
(42) Poulsen, I. A.; Garner, C. S. *J. Am. Chem. Soc.* **1962**, *84*, 2032–2037.
(43) The perchlorate salt was prepared by modifying the synthetic procedure for preparing the bromide salt (procedure B) as described in: Jackels, S. C.; Farmery, K.; Barefield, E. K.; Rose, N. J.; Busch, D. H. *Inorg. Chem.* **1972**, *11*, 2893–2901.
(44) Ford-Smith, M. H.; Sutin, N. *J. Am. Chem. Soc.* **1961**, *83*, 1830–1834.
(45) Brown, G. M.; Sutin, N. *J. Am. Chem. Soc.* **1979**, *101*, 883–892. In the modified approach used in this work to estimate a_i and a_j values, the orthoganol axes selected for measurement were chosen so that one axis represented the minimum possible contact distance for the complex.

Table II. Formal Electrode Potentials and Self-Exchange Rate Constants for Counterreagents Utilized in This Work at 25 °C, μ = 0.10 M

reagent system	E^f (vs. NHE), V	k_{ex}, M^{-1} s^{-1}	contact radius (a_i), nm
$Fe(phen)_3^{3+/2+}$	1.098[a]	3.3×10^8 [b]	0.63
$Fe(bpy)_3^{3+/2+}$	1.099[c]	3.3×10^8 [b]	0.60
$Fe(4,7\text{-}Me_2phen)_3^{3+/2+}$	0.939[d]	3.3×10^8 [b]	0.66
$IrCl_6^{2-/3-}$	0.892[e]	2.3×10^5 [f]	0.47
$Co(Me_4[14]tetraeneN_4)^{3+/2+}$	0.562[j]	5.0×10^{-3} [h]	0.47
$Ru(NH_3)_4bpy^{3+/2+}$	0.526[i]	2.2×10^6 [j]	0.44

[a] As determined in this work: E^f = 1.098 ± 0.003 V (0.10 M CF_3SO_3H); E^f = 1.112 ± 0.002 V (0.05 M KCl); the latter value compares favorably with the literature value of 1.117 V.[48] [b] Reference 49 (but see text). [c] As determined in this work: E^f = 1.099 ± 0.003 V (0.10 M CF_3SO_3H); E^f = 1.092 ± 0.003 V (0.05 M KCl); the latter value agrees with the literature value.[48] [d] As determined in this work: E^f = 0.939 ± 0.001 V (0.05 M KCl); same value assumed applicable to 0.10 M CF_3SO_3H by analogy to other iron–polypyridyl reagents (see text). [e] For 0.10 M $NaClO_4$.[50] [f] Reference 51. [g] For 0.10 M $HClO_4$.[48] [h] Corrected to 0.10 M $HClO_4$ from value determined in 1.0 M $HClO_4$.[52] [i] For 0.10 M ionic strength, medium unspecified.[53] [j] Reference 45.

$E_{1/2}$ values as determined from slow-scan cyclic voltammetric measurements[46] using a graphite rod electrode to minimize surface adsorption. Due to limited solubility, the $E_{1/2}$ value for $Cu(Et_2\text{-}2,3,2\text{-}S_4)^{2+/+}$ could not be determined satisfactorily in aqueous solution but was assumed to have the same value as measured for $Cu(Me_2\text{-}2,3,2\text{-}S_4)^{2+/+}$ by analogy to their similar behavior in 80% methanol.[47] The aqueous E^f values for all Cu(II)/(I) systems are listed in Table I.

In view of the relatively large potentials of the copper–polythia ethers, it was necessary to select an oxidizing agent of equivalent or larger potential for the oxidation kinetic studies. The iron(III)/iron(II)–polypyridyl systems appeared to be the most promising candidates, but their large self-exchange rate constants, in conjunction with their large potential values, suggested that some of the cross-exchange rates with Cu^IL species might exceed the time domain of the stopped-flow technique.

On the basis of these considerations, $Fe(4,7\text{-}Me_2phen)_3^{3+/2+}$ was selected in view of its lower potential value. However, the absence of a suitable literature value required that the potential be determined as part of this work. Due to the low solubility of this system in 0.10 M CF_3SO_3H (the medium used for the kinetic studies), the cyclic voltammetric $E_{1/2}$ values of $Fe(phen)_3^{3+/2+}$, $Fe(bpy)_3^{3+/2+}$, and $Fe(4,7\text{-}Me_2phen)_3^{3+/2+}$ were first determined in 0.05 M KCl for comparison to available literature data,[48] and then the former two systems were remeasured in 0.10 M CF_3SO_3H. The similarity of the $E_{1/2}$ values measured for $Fe(phen)_3^{3+/2+}$ and $Fe(bpy)_3^{3+/2+}$ in these two media indicated that the value measured directly for $Fe(4,7\text{-}Me_2phen)_3^{3+/2+}$ in 0.05 M KCl could be applied to 0.10 M CF_3SO_3H. The potential values for all three iron systems are listed in Table II along with literature values for the other reagents utilized in this work.

Oxidation Kinetics Using $Fe^{III}(4,7\text{-}Me_2phen)_3$. As noted above, the oxidation kinetics of the Cu(I)–polythia ether complexes were studied by using $Fe^{III}(4,7\text{-}Me_2phen)_3$ (abbreviated subsequently as $Fe^{III}Z_3$) as the oxidizing agent based on its several favorable properties including (i) a formal potential value (E^f = 0.939 V) sufficiently high to promote the quantitative oxidation of all Cu^IL species, particularly under conditions where one reagent is present in large excess; (ii) a constrained coordination geometry that promotes reaction by outer-sphere electron-transfer pathways; (iii) a presumed knowledge of the self-exchange rate constant;[49] and (iv) a large visible absorption peak for the $Fe^{II}Z_3$ product (λ = 512 nm, ϵ = 14 000) suitable for monitoring the electron-transfer reactions. The cross-reactions studied were of the type

$$Cu^IL + Fe^{III}Z_3 \xrightarrow{k_{31}} Cu^{II}L + Fe^{II}Z_3 \qquad (3a)$$

where k_{31} represents the second-order rate constant for the electron-transfer reaction in accordance with the differential expression

$$\frac{d[Fe^{II}Z_3]}{dt} = k_{31}[Cu^IL][Fe^{III}Z_3] \qquad (4)$$

The kinetic studies were carried out in 0.10 M CF_3SO_3H (since $Fe^{III}Z_3$ is very insoluble in 0.10 M $HClO_4$) under pseudo-first-order conditions in which the Cu^IL species were present in large excess. The kinetic data were then treated according to the integrated expression

$$\ln (A_\infty - A_t) = -k_{app}t + \ln (A_\infty - A_0) \qquad (5)$$

where A_0, A_t, and A_∞ represent the measured absorbance values at the time of reaction initiation, at any time, t, and at infinite time (final equilibrium), respectively, and

$$k_{app} = k_{31}[Cu^IL]_0 \qquad (6)$$

In general, several kinetic runs were made with varying initial concentrations of the Cu^IL complex, $[Cu^IL]_0$, and linear regression analysis was used to establish the best value of k_{31}. In the case of the $[12]aneS_4$ system, the limited solubility of this polythia ether ligand restricted the maximum value of $[Cu^IL]_0$ that could be easily obtained and only initial rates were measured in many instances to avoid violating pseudo-first-order conditions. For the $[13]aneS_4$ system, only one set of conditions was utilized. For all other systems, between four and eight values of $[Cu^IL]_0$ were included covering at least a 10-fold range.

The reaction of $Fe^{III}Z_3$ with $Cu^I([15]aneS_5)$ was very rapid at 25 °C necessitating the utilization of very dilute solutions. This enhanced the possibility of error in the observed k_{app} values for this system.

The $Fe^{III}Z_3$ reagent tended to undergo partial reduction prior to the initiation of the cross-reactions. By the utilization of pseudo-first-order conditions in which Cu^IL was present in considerable excess, however, an exact knowledge of the initial

Table III. Resolved Cross-Reaction Rate Constants for the Oxidation of Copper(I)–Polythia Ether Complexes by $Fe^{III}(4,7\text{-}Me_2phen)_3$ in 0.10 M CF_3SO_3H

complexed ligand	temp, °C	$10^{-6}k_{31}$, M^{-1} s^{-1}	ΔH^* kJ mol^{-1}	ΔS^*, J K^{-1} mol^{-1}
$[12]aneS_4$	25.0	1.2 ± 0.4		
$[13]aneS_4$	25.0	1.8		
$[14]aneS_4$	5.5	2.37 ± 0.12	33.9 ± 0.8	2.5 ± 2.1
	15.0	4.01 ± 0.27		
	25.0	9.9 ± 0.3		
		6.6 ± 0.6		
$[15]aneS_4$	25.0	15.4 ± 0.1		
$[16]aneS_4$	25.0	2.5 ± 0.1		
$Me_2\text{-}2,3,2\text{-}S_4$	25.0	0.0473 ± 0.0005		
$Et_2\text{-}2,3,2\text{-}S_4$	5.5	0.0118 ± 0.0002	33.1 ± 6.3	−46 ± 2.1
	15.0	0.0228 ± 0.0003		
	25.0	0.0318 ± 0.0005		
$[15]aneS_5$	5.5	25.2 ± 1.1	19.7 ± 0.8	−29 ± 21
	15.0	35 ± 5		
	25.0	46 ± 4		
		47 ± 9		

(46) Rorabacher, D. B.; Martin, M. J.; Koenigbauer, M. J.; Malik, M.; Schroeder, R. R.; Endicott, J. F.; Ochrymowyz, L. A. In *Copper Coordination Chemistry: Biochemical and Inorganic Perspectives*; Karlin, K. D., Zubieta, J., Eds.; Adenine: Guilderland, NY, 1983; pp 167–202.
(47) Dockal, E. R.; Jones, T. E.; Sokol, W. F.; Engerer, R. J.; Rorabacher, D. B.; Ochrymowycz, L. A. *J. Am. Chem. Soc.* **1976**, *98*, 4322–4324.
(48) Yee, E. L.; Cave, R. J.; Guyer, K. L.; Tyma, P. D.; Weaver, M. J. *J. Am. Chem. Soc.* **1980**, *101*, 1131–1132.
(49) The self-exchange rate constant value for $Fe(4,7\text{-}Me_2phen)_3^{3+/2+}$ is generally assumed to be identical with the value reported for $Fe(phen)_3^{3+/2+}$: Ruff, I.; Zimonyi, M. *Electrochim. Acta* **1973**, *18*, 515–516.
(50) Margerum, D. W.; Chellappa, K. L.; Bassu, F. P.; Bruce, G. L. *J. Am. Chem. Soc.* **1975**, *97*, 6894–6896.
(51) Hurwitz, P.; Kustin, K. *Trans. Faraday Soc.* **1966**, *62*, 427–432.
(52) Durham, B. Ph.D. Dissertation, Wayne State University, 1977.
(53) Yee, E. L.; Weaver, M. J. *Inorg. Chem.* **1980**, *19*, 1077–1079.

concentration of $Fe^{III}Z_3$ was not essential. Nonetheless, the initial concentration was frequently estimated by comparing the difference in the initial and final absorbances attributable to $Fe^{II}Z_3$.

The activation parameters associated with reaction 3a were evaluated for the Cu(I) complexes with [14]aneS$_4$, Et$_2$-2,3,2-S$_4$, and [15]aneS$_5$ from kinetic measurements at 5.5, 15.0, and 25.0 °C. These systems were selected as those having the smallest and largest formal potentials and the largest apparent self-exchange rate constant, respectively.

The resolved cross-reaction rate constants for all Cu(I) complexes reacting with $Fe^{III}Z_3$, along with activation parameters where applicable, are listed in Table III.

Reduction Kinetics Using $Co^{II}(Me_4[14]tetraeneN_4)(H_2O)_2$. The $Co^{II}(Me_4[14]tetraeneN_4)(H_2O)_2$ complex (subsequently abbreviated as $Co^{II}N_4$) was selected as the reducing agent for the $Cu^{II}L$ complexes in the kinetic studies on the basis of its several favorable properties including (i) a formal potential value ($E^f = 0.562$ V)[54] capable of reducing all of the Cu(II) species of interest, (ii) an established self-exchange rate constant,[52] (iii) demonstrated outer-sphere electron-transfer behavior in its reactions with related diaquo(macrocyclic tetramine)cobalt(III) complexes,[52] and (iv) a sufficiently large molar absorptivity value in the visible region ($\lambda = 540$ nm, $\epsilon = 3150$) that the progress of its reactions could be monitored spectrophotometrically.

All of the reactions studied were of the type

$$Cu^{II}L + Co^{II}N_4 \xrightarrow{k_{12}} Cu^{I}L + Co^{III}N_4 \qquad (2a)$$

where k_{12} represents the cross-reaction rate constant of interest. The reactions were actually monitored at 510 nm (where $\epsilon = 2440$ for $Co^{II}N_4$) to circumvent the large absorbance of many of the $Cu^{II}L$ complexes at 540 nm.

Since the $Cu^{II}L$ complexes have small stability constants[55] and, thus, were only partially formed under the reaction conditions utilized, a significant quantity of uncomplexed aquocopper(II) ion was always present in the $Cu^{II}L$ solutions. The possibility that the aquocopper(II) ion might provide a competing pathway for electron transfer from $Co^{II}N_4$ (eq 7) was independently investigated.

$$Cu^{II}(aq) + Co^{II}N_4 \underset{k_{41}}{\overset{k_{14}}{\rightleftharpoons}} Cu^{I}(aq) + Co^{III}N_4 \qquad (7)$$

In view of the fact that the direct reaction of $Cu^{II}(aq)$ with $Co^{II}N_4$ is not thermodynamically favorable, the reverse reaction was studied. The $Cu^{I}(aq)$ solutions were prepared by reacting an aqueous solution of $Cu(ClO_4)_2$ with a less than stoichiometric amount of $Cr(ClO_4)_2$ under deaerated conditions. The resulting $Cu^{I}(aq)$ solution was withdrawn with a gastight syringe fitted with a Teflon needle and immediately inserted into the stopped-flow spectrophotometer for kinetic measurements. By the utilization of pseudo-first-order conditions with $Co^{III}N_4$ in large excess, it was unnecessary to determine the Cu(I) concentration accurately. On the basis of 13 different combinations of reactant concentrations (with 2–5 runs each), a value of $k_{41} = 4.3\ (\pm 0.5) \times 10^4$ M^{-1} s^{-1} was obtained in 0.10 M $HClO_4$ at 25 °C. With this value and the calculated equilibrium constant for reaction 7,[56] the calculated value for k_{14} was obtained as

$$k_{14} = \frac{k_{41}}{K_{41}} = \frac{4.3 \times 10^4}{8.3 \times 10^6} = 5.2 \times 10^{-3}\ M^{-1}\ s^{-1} \qquad (8)$$

This latter value is 4–7 orders of magnitude smaller than the cross-reaction rate constants observed for reaction 2a (see below) indicating that reaction 7 is not a competing pathway in the reduction of the various $Cu^{II}L$ species by $Co^{II}N_4$.

Table IV. Resolved Cross-Reaction Rate Constants for Reduction of Copper(II)–Polythia Ether Complexes by $Co^{II}(Me_4[14]tetraeneN_4)(OH_2)_2$ at 25.0 °C, $\mu = 0.10$ M ($HClO_4$)

complexed ligand	$10^{-1}k_{12}$, M^{-1} s^{-1}	complexed ligand	$10^{-1}k_{12}$, M^{-1} s^{-1}
H_2O	0.0045[a]	[15]aneS$_4$	21.9 ± 0.09.
[12]aneS$_4$	21.2 ± 1.2	[16]aneS$_4$	5.3
	26.6 ± 1.7	Me$_2$-2,3,2-S$_4$	485 ± 13
[13]aneS$_4$	5.0 ± 0.2	Et$_2$-2,3,2-S$_4$	256 ± 49
[14]aneS$_4$	0.75 ± 0.04[b]	[15]aneS$_5$	58.8 ± 0.2
	0.70 ± 0.02[b]		
	0.67 ± 0.02[c]		

[a] Rate constants for $Cu(aq)^{2+}$ estimated from oxidation of $Cu(aq)^{+}$ by $Co^{III}N_4$ at pH 1.0 (see text). [b] Determined at pH 1.0 (0.10 M $HClO_4$). [c] Determined at pH 2.0 (0.01 M $HClO_4$ + 0.09 M $LiClO_4$).

The kinetics of reaction 7 were also measured at pH 2.0 (0.01 M $HClO_4$, 0.09 M $LiClO_4$) yielding $k_{41} = 3.32\ (\pm 0.09) \times 10^5$ M^{-1} s^{-1}. The nearly 10-fold increase in the k_{41} value compared to the study at pH 1.0 suggests that reaction 7 proceeds by an inner-sphere mechanism involving a hydroxide-bridged intermediate (and, therefore, could interfere at pH >5).

In view of the pH dependence observed for reaction 7, the possibility of a similar pH dependence for reaction 2a was also investigated. The values obtained for $Co^{II}N_4$ reacting with Cu^{II}([14]aneS$_4$) were $k_{12} = 7.5\ (\pm 0.4)$ and $7.0\ (\pm 0.2)$ M^{-1} s^{-1} (duplicate runs) at pH 1.00 and $k_{12} = 6.7\ (\pm 0.2$ M^{-1} s^{-1} at pH 2.00. Thus, a hydroxide-bridged inner-sphere mechanism does not appear to be implicated in reaction 2a.

For all eight polythia ether complexes, the reaction kinetics conformed to the second-order expression (independent of pH)

$$\frac{-d[Co^{II}N_4]}{dt} = k_{12}[Co^{II}N_4][Cu^{II}L] \qquad (9)$$

These reactions were also studied under pseudo-first-order conditions where $[Cu^{II}L] \gg [Co^{II}N_4]$ to yield the observed rate expression

$$\frac{-d[Co^{II}N_4]}{dt} = k_{app}[Co^{II}N_4] \qquad (10)$$

Since the $Cu^{II}L$ species were generally partially dissociated (even in the presence of excess $Cu^{II}(aq)$), the actual concentration of $Cu^{II}L$ (i.e., $[Cu^{II}L]_0$) was generally determined spectrophotometrically.[55] Under the reaction conditions used, the $[Cu^{II}L]/[Cu^{II}(aq)]$ ratio did not change significantly during the course of the reaction. Thus, the observed reaction kinetics followed eq 5, and the k_{12} values were readily obtained by linear regression analysis of eq 11.

$$k_{app} = k_{12}[Cu^{II}L]_0 \qquad (11)$$

Due to solubility limitations, the system involving [16]aneS$_4$ was studied under only one set of concentration conditions. As a result, the k_{12} value for this latter system is less well defined.

The resolved k_{12} values for all $Cu^{II}L$ species reacting with $Co^{II}N_4$ are given in Table IV.

Reduction Kinetics of $Cu^{II}L$ Species with $Ru^{II}(NH_3)_4bpy$. As an independent check on the cross-reaction kinetic data obtained for reaction 2a, the reduction kinetics for a few of the $Cu^{II}L$ complexes were studied by using $Ru^{II}(NH_3)_4bpy$ as the reducing agent:

$$Cu^{II}L + Ru^{II}(NH_3)_4bpy \xrightarrow{k_{15}} Cu^{I}L + Ru^{III}(NH_3)_4bpy \qquad (12)$$

For these studies, the Cu(II) complexes with [14]aneS$_4$, Et$_2$-2,3,2-S$_4$, and [15]aneS$_5$ were selected as these represent the systems with the largest and smallest formal potential values and the largest apparent self-exchange rate constant, respectively. (These are also the only systems for which structural information on the $Cu^{I}L$ species is available.)[39,40]

The reactions were monitored by following the loss of $Ru^{II}(NH_3)_4bpy$ at 295 nm ($\epsilon = 32\,000$). For the reaction with Cu^{II}([14]aneS$_4$), the kinetics were studied under pseudo-first-order

(54) Chou, M.; Creutz, C.; Sutin, M. *J. Am. Chem. Soc.* **1977**, *99*, 5615–5623.
(55) Sokol, L. S. W. L.; Ochrymowycz, L. A.; Rorabacher, D. B. *Inorg. Chem.* **1981**, *20*, 3189–3195.
(56) The value of K_{41} was calculated from eq 20 by using $E_{44}{}^f = 0.562$ V for $CoN_4^{3+/2+}$ (Table II) and $E_{11}{}^f = 0.153$ V for $Cu(aq)^{2+/+}$: Latimer, W. M. *The Oxidattion States of the Elements and Their Potentials in Aqueous Solution*: 2nd ed.: Prentice-Hall: Englewood Cliffs, NJ, 1952; p 186).

Table V. Resolved Cross-Reaction Rate Constants for the Reduction of Selected Copper(II)–Polythia Ether Complexes by $Ru^{II}(NH_3)_4bpy$ at 25.0 °C, Variable Perchlorate Ion Concentration

complexed ligand	$[HClO_4]$, M	$10^{-6}k_{15}$, M^{-1} s^{-1}
[14]aneS$_4$	0.025	0.266 ± 0.006
	0.050	0.351 ± 0.007
	0.10	0.480 ± 0.004
	0.50	1.05 ± 0.03
Et$_2$-2,3,2-S$_4$	0.10	>100
[15]aneS$_5$	0.10	84 ± 15

Table VI. Resolved Cross-Reaction Rate Constants for the Oxidation of $Cu^{I}(Et_2\text{-}2,3,2\text{-}S_4)$ with $Fe^{III}(phen)_3$ and $Fe^{III}(bpy)_3$ in 0.10 M CF_3SO_3H

reagent	temp, °C	$10^{-6}k_{31}$, M^{-1} s^{-1}	$\Delta H^{\ddagger}$, kJ mol^{-1}	$\Delta S^{\ddagger}$, J K^{-1} mol^{-1}
$Fe^{III}(bpy)_3$	25.0	0.0621 (±0.0017)		
$Fe^{III}(phen)_3$	5.5	0.492 (±0.004)	~27[a]	~−36[a]
	15.0	0.746 (±0.014)		
	25.0	0.247 (±0.003) (?)		
	[25.0	1.1][b]		

[a] Approximate activation parameters based on 5.5 and 15.0 °C data only. [b] Extrapolated 25 °C value of k_{31} based on 5.5 and 15.0 °C data.

conditions with $Cu^{II}L$ present in large excess. The kinetics of this specific reaction were also investigated as a function of $HClO_4$ concentration over a 20-fold range: 0.025, 0.050, 0.10, and 0.50 M.

In the case of the $Cu^{II}([15]aneS_4)$ complex, the reaction with $Ru^{II}(NH_3)_4bpy$ was too fast to be studied under pseudo-first-order conditions at detectable concentration levels. Therefore, this reaction was studied as a second-order process at 0.10 M $HClO_4$. Under the conditions used in this study, the rate of the electron-transfer reaction was five to six times faster than the formation of the $Cu^{II}L$ complex from its dissociated constituents, $Cu(aq)^{2+}$ and L.[41] Thus, to a good approximation, only the $Cu^{II}L$ initially present contributed to the observed reaction kinetics for reaction 12 over the first 50% of the reaction.

An attempt was made to study the kinetics of $Cu^{II}(Et_2\text{-}2,3,2\text{-}S_4)$ reacting with $Ru^{II}(NH_3)_4bpy$ under second-order conditions as well. However, within the accessible concentration range that could be detected, this reaction proved to be too fast to be monitored by the stopped-flow method, suggesting that $k_{15} > 10^8$ M^{-1} s^{-1}.

The k_{15} values determined for these systems are recorded in Table V.

Oxidation Kinetics of $Cu^{I}L$ Species with $Fe^{III}(phen)_3$ and $Fe^{III}(bpy)_3$. As a check on the cross-reaction kinetic data obtained for reaction 3a, the oxidation kinetics of $Cu^{I}(Et_2\text{-}2,3,2\text{-}S_4)$ were studied by using $Fe^{III}(phen)_3$ and $Fe^{III}(bpy)_3$ as oxidizing agents. (Because of the large potential values and self-exchange rate constants of these latter reagents, only the open-chain ligand complexes of Cu(I) were predicted to have cross-reaction rates that were within the stopped-flow time domain.) The reaction conditions and data treatment were identical with those for the $Fe^{III}Z_3$ study. The resolved cross-reaction rate constant (k_{31}) values are listed in Table VI.

Oxidation Kinetics Using $IrCl_6^{2-}$. In a separate study, the kinetics of oxidation of $Cu^{I}([14]aneS_4)$ and $Cu^{I}(Me_2\text{-}2,3,2\text{-}S_4)$ by $IrCl_6^{2-}$ were investigated. The $IrCl_6^{2-}$ oxidant was generated photochemically by flash photolysis of an $IrCl_6^{3-}$ solution as described by the following sequence of reactions:

$$IrCl_6^{3-} \xrightarrow{h\nu} IrCl_6^{2-} + e^- \text{ (fast)} \quad (13)$$

$$H^+ + e^- \rightarrow H^\bullet \text{ (fast)} \quad (14)$$

$$H^\bullet + H^\bullet \rightarrow H_2 \text{ (fast)} \quad (15)$$

$$Cu^{I}L + IrCl_6^{2-} \xrightarrow{k_{61}} Cu^{II}L + IrCl_6^{3-} \quad (16)$$

The outer jacket of the flash photolysis cell was filled with 1 M HBr, which served as an absorbing filter to remove higher energy radiation with a sharp cutoff at 230 nm.

By the utilization of 4×10^{-4} M $IrCl_6^{3-}$ in the flash photolysis cell, a single 200-J (8-kV) flash produced 1.2×10^{-6} M $IrCl_6^{2-}$ (0.3% conversion). The $IrCl_6^{2-}$ immediately reacted with $Cu^{I}L$ to produce $Cu^{II}L$ (eq 16) as observed by monitoring either the decrease in absorbance of $IrCl_6^{2-}$ at 487 nm (ϵ = 4050) or, in the case of the [14]aneS$_4$ system, the increase in absorbance of $Cu^{II}L$ at 390 nm (ϵ = 8040). By monitoring the latter wavelength, we could subsequently observe the initially generated $Cu^{II}([14]aneS_4)$ to dissociate to $Cu(aq)^{2+}$ and free [14]aneS$_4$. For the Me$_2$-2,3,2-S$_4$ system, however, the dissociation of the $Cu^{II}L$ complex could not be observed as a separate step. This is consistent with the fact that this open-chain complex is known to dissociate 4000 times faster than $Cu^{II}([14]aneS_4)$.[41]

The observed cross-reaction rate constants for both reactions studied with $IrCl_6^{2-}$ are listed in Table VII.

Kinetics of $Co^{II}(Me_4[14]tetraeneN_4)$ Reacting with $Fe^{III}(4,7\text{-}Me_2phen)_3$. Since $Co^{II}(Me_4[14]tetraeneN_4)$ and $Fe^{III}(4,7\text{-}Me_2phen)_3$ were the primary cross-reaction electron-transfer reagents utilized in this study, the kinetics of the electron-transfer between these two reagents were studied to determine the internal consistency of the formal potential values and apparent self-exchange rate constants for their respective redox couples. Reaction 17 was studied at 5.5, 15.0, and 25.0 °C in 0.10 M CF_3SO_3H

$$Co^{II}N_4 + Fe^{III}Z_3 \xrightarrow{k_{32}} Co^{III}N_4 + Fe^{II}Z_3 \quad (17)$$

under pseudo-first-order conditions with $Co^{II}N_4$ present in large excess. The progress of this reaction was monitored by following the increase in absorbance of $Fe^{II}Z_3$ at 440 nm (ϵ = 8615). The resulting k_{32} values are given in Table VIII.

Table VII. Apparent Cross-Reaction Rate Constants for the Oxidation of Copper(I)–Polythia Ether Species by Flash-Generated Hexachloroiridate(IV) Ion at 25 °C, μ = 0.10 M ($HClO_4$)

complexed ligand	$10^{-8}k_{51}$, M^{-1} s^{-1}
[14]aneS$_4$	2.1 (±0.1)[a]
Me$_2$-2,3,2-S$_4$	≥1.3

[a] When the subsequent decay of the $Cu^{I}([14]aneS_4)$ product was monitored, a dissociation rate constant of k_d = 11 s^{-1} obtained which compares favorably with an indirect estimate of k_f = 6 s^{-1}.[41]

Table VIII. Resolved Cross-Reaction Rate Constants for the Reaction of $Co^{II}(Me_4[14]tetraeneN_4)(OH_2)_2$ with $Fe^{III}(4,7\text{-}Me_2phen)_3$ as a Function of Temperature in 0.10 M CF_3SO_3H

temp, °C	$10^{-4}k_{32}$, M^{-1} s^{-1}
5.5	4.36 (±0.06)
15.0	6.15 (±0.33)
25.0	7.96 (±0.17)

$\Delta H^{\ddagger}$ = 18.8 (±1.7) kJ mol^{-1}

$\Delta S^{\ddagger}$ = −79 (±5) J K^{-1} mol^{-1}

Discussion

Calculation of Apparent Self-Exchange Rate Constants. Concerns about the applicability of the Marcus cross-relation to reactions of low molecular weight copper complexes have already been noted in the Introduction. Nonetheless, since most previous kinetic studies on Cu(II)/(I) electron-transfer processes have been analyzed by this approach, its application to the current systems to obtain *apparent* self-exchange rate constants provides a method for comparing the relative reactivity of the copper–polythia ether complexes to previously studied systems.

As applied specifically to reactions 2a and 3a, the classical Marcus cross-relations may be formulated respectively as

$$k_{12} = (k_{11}k_{22}K_{12}f_{12})^{1/2}W_{12} \quad (18)$$

$$k_{31} = (k_{11}k_{33}K_{31}f_{31})^{1/2}W_{31} \quad (19)$$

where k_{11}, k_{22}, and k_{33} represent the outer-sphere self-exchange

Table IX. Calculated Self-Exchange Rate Constants for Copper(II)/Copper(I)–Polythia Ether Systems at 25 °C, $\mu = 0.10$

complexed ligand	calcd $k_{11}(Ox)^a$	calcd $k_{11}(Red)^b$	$k_{11}(Red)/k_{11}(Ox)$	calcd $\bar{k}_{11}{}^c$	calcd $k_{11}(comb)^d$
[12]aneS$_4$	1.0×10^{-2}	3.1×10^5	3×10^7	5.6×10	1.6×10^2
		4.9×10^5	5×10^7	7.0×10	2.0×10^2
[13]aneS$_4$	5.2×10^{-2}	1.0×10^5	2×10^6	7.2×10	2.3×10^2
[14]aneS$_4$	2.2	1.6×10^3	7×10^2	5.9×10	4.7×10
	0.93		17×10^2	3.9×10	3.0×10
		$[2.8 \times 10^3]^e$			
[15]aneS$_4$	1.4×10	5.0×10^3	4×10^2	2.6×10^5	2.2×10^2
[16]aneS$_4$	2.0×10	3.7×10^3	2×10^3	8.6×10	7.8×10
Me$_2$-2,3,2-S$_4$	6.4×10^{-2}	1.7×10^5	3×10^6	1.0×10^2	2.5×10^2
Et$_2$-2,3,2-S$_4$	2.9×10^2	4.6×10^4	2×10^6	3.7×10	8.5×10
	$[0.04 \times 10^{-2}]^f$				
	$[0.83 \times 10^{-2}]^g$				
	$[15 \times 10^{-2}]^h$				
[15]aneS$_5$	7.4×10^3	3.5×10^5	5×10	5.1×10^4	1.7×10^4
	7.7×10^3		5×10	5.2×10^4	1.8×10^4
		$[2.4 \times 10^5]^e$			

[a] Unless otherwise noted, $k_{11}(Ox)$ values are calculated from the cross-reaction of $Fe^{III}Z_3$ with the $Cu^{I}L$ complexes by using eq 18. [b] Unless otherwise noted, $k_{11}(Red)$ values are calculated from the cross-reaction of $Co^{II}N_4$ with the $Cu^{II}L$ complexes by using eq 19. [c] $\bar{k}_{11}$ represents the geometric mean of $k_{11}(Ox)$ and $k_{11}(Red)$ as calculated from the cross-reactions with $Fe^{III}Z_3$ and $Co^{II}N_4$. [d] $k_{11}(comb)$ values are calculated from the simultaneous solution of eq 18 and 19 using experimental rate constants from the cross-reactions with both $Fe^{III}Z_3$ and $Co^{II}N_4$. [e] Calculated from the cross-reaction of $Ru^{II}(NH_3)_4bpy$ with the $Cu^{II}L$ complexes. [f] Calculated from the cross-reaction of $Fe^{III}(bpy)_3$ with the $Cu^{I}L$ complex. [g] Calculated from the experimental cross-reaction rate constants at 25 °C for the reaction of $Fe^{III}(phen)_3$ with $Cu^{I}(Et_2\text{-}2,3,2\text{-}S_4)$. [h] Calculated from the extrapolated cross-reaction rate constant at 25 °C as determined from 5.5 and 15 °C experimental rate constants for the reaction of $Fe^{III}(phen)_3$ with $Cu^{I}(Et_2\text{-}2,3,2\text{-}S_4)$.

rate constants for $CuL^{2+/+}$, $CoN_4{}^{3+/2+}$, and $FeZ_3{}^{3+/2+}$, respectively, and the other terms may be calculated from the relationships 20–24. In the latter equations, $E_{ii}{}^f$ and $E_{jj}{}^f$ represent the formal

$$\ln K_{ij} = (E_{ii}{}^f - E_{jj}{}^f)nF/RT \tag{20}$$

$$\ln f_{ij} = \frac{1}{4}(\ln K_{ij} + \delta_{ij} - \delta_{ji})^2 \Big/ \left[\ln \left(\frac{k_{ii}k_{jj}}{A_{ii}A_{jj}} \right) + \delta_{ii} + \delta_{jj} \right] \tag{21}$$

$$\ln W_{ij} = \tfrac{1}{2}(-\delta_{ij} - \delta_{ji} + \delta_{ii} + \delta_{jj}) \tag{22}$$

$$\delta_{ij} = \frac{Z_i Z_j e_0{}^2}{D k_B T}\left(\frac{1}{a'} - \frac{\kappa}{1 + \kappa a'} \right) \tag{23}$$

$$\kappa = \left(\frac{8\pi N_A e_0{}^2 \mu}{10000 D k_B T} \right)^{1/2} \tag{24}$$

potentials of the redox couples for the reacting oxidant and reductant, respectively, for rate constant k_{ij} (thus, in our numbering scheme, $E_{11}{}^f$, $E_{22}{}^f$, and $E_{33}{}^f$ are the formal potentials for $CuL^{2+/+}$, $CoN_4{}^{3+/2+}$ and $FeZ_3{}^{3+/2+}$, respectively), n is the number of electrons transferred, F is the Faraday constant, R is the gas constant, T is the absolute temperature, A_{ii} and A_{jj} are the preexponential factors for the respective self-exchange reactions (their product being approximated as 10^{22} M^{-2} s^{-2} in this work), Z_i and Z_j are the formal charges on the reacting partners involved in k_{ij}, e_0 is the electronic charge, D is the static dielectric constant of the solvent, k_B is the Boltzmann constant, $a' = a_i + a_j$ where a_i and a_j are the outer-sphere contact radii (in cm) of the reacting partners, N_A is Avogadro's number, and μ is the ionic strength.

In the selection of appropriate values for outer-sphere contact radii (a_i, a_j), a modification of the method employed by Brown and Sutin was utilized.[45] A contact radius of 0.44 nm was estimated for the copper–polythia ether complexes by this method, and the corresponding values for all other reagents are included in Table II. These distance parameters, along with the respective potential values (using the measured $E_{1/2}$ values for the copper complexes) and self-exchange rate constants (as listed in Tables I and II) were substituted into eq 18 and 19 to yield the apparent k_{11} values for $Cu^{I}L$ oxidation ($k_{11}(Ox)$) and $Cu^{II}L$ reduction ($k_{11}(Red)$), respectively. These calculated values are listed in Table IX.

As observed previously in the case of the copper–polypyridyl complexes,[28a,35] the $k_{11}(Ox)$ and $k_{11}(Red)$ values for most of the copper–polythia ethers tend to differ by several orders of magnitude, but the ratio is reversed for the polythia ether complexes relative to those of previously studied copper systems (i.e., $k_{11}(Red) \gg k_{11}(Ox)$). In the most extreme cases, the $k_{11}(Red)/k_{11}(Ox)$ ratio exceeds 10^6 for the two smallest macrocyclic ligand systems and the two open-chain ligand systems.

Lee and Anson's hypothesis that the differing $k_{11}(Ox)$ and $k_{11}(Red)$ values may reflect a difference in reorganizational energy contributions of $Cu^{II}L$ and $Cu^{I}L$ suggests that the geometric mean self-exchange rate constants, designated here as $\bar{k}_{11}$ (eq 25), may

$$\bar{k}_{11} = (k_{11}(Ox)k_{11}(Red))^{1/2} \tag{25}$$

be more representative of the overall electron-transfer reactivity of these systems. Despite the huge fluctuations in the individual $k_{11}(Ox)$ and $k_{11}(Red)$ values, the geometric mean values (Table IX) for all of the copper-tetrathia ether complexes are within the same order of magnitude. This observation is particularly surprising since the ligands included in this study cover a wide range of flexibility from the relatively rigid small macrocycles ([12]aneS$_4$, [13]aneS$_4$) to the very flexible open-chain ligands (Me$_2$-2,3,2-S$_4$, Et$_2$-2,3,2-S$_4$). Only in the case of the pentathia ether system, $Cu([15]aneS_5)^{2+/+}$, does the $\bar{k}_{11}$ value differ significantly, being approximately 10^3 greater than for the other seven systems.

Serious discussion of the significance of self-exchange rate constants resolved by the foregoing approach is precluded by (i) the lack of an obvious physical meaning for the geometric mean of $k_{11}(Red)$ and $k_{11}(Ox)$ when these quantities differ by several orders of magnitude and (ii) the probability that $\bar{k}_{11}$ does not adequately represent a reaction coordinate in which there are changes in coordination number. Subsequent to a brief consideration of some potential sources of error in the individual k_{11} values, as outlined below, a more logical model of the reaction coordinate is proposed that could account for the variable discrepancies in the $k_{11}(Red)$ and $k_{11}(Ox)$ values.

Internal Consistency of Electron-Transfer Parameters. The validity of the calculated k_{11} values listed in Table IX is dependent upon the accuracy of the self-exchange rate constants and formal potentials for both $CoN_4{}^{3+/2+}$ and $FeZ_3{}^{3+/2+}$ (i.e., k_{22}, k_{33}, $E_{22}{}^f$ and $E_{33}{}^f$). This point is of particular concern since the k_{22} (k_{ex}) value for $CoN_4{}^{3+/2+}$ was corrected from literature data obtained at higher ionic strength[52] and the k_{33} value for $FeZ_3{}^{3+/2+}$ was assumed to be equal to that determined experimentally for a related system, $Fe(phen)_3{}^{3+/2+}$.[49]

Using the electron-transfer parameters for these two reagent systems (as listed in Table II) and substituting these values into

the appropriate form of the Marcus equation yields a calculated rate constant for the cross reaction between $Fe^{III}Z_3$ and $Co^{II}N_4$ (eq 17) of $k_{32} = 9.6 \times 10^5$ M^{-1} s^{-1} at 25 °C. This value is 1 order of magnitude larger than the experimentally determined value of 8.0×10^4 M^{-1} s^{-1} (Table VIII). Whereas such discrepancies are sometimes observed in Marcus calculations, this level of disagreement suggests the possibility that either (i) some of the parameters for $FeZ_3^{3+/2+}$ and/or $CoN_4^{3+/2+}$, as listed in Table II, are in error or (ii) the reactions of $CoN_4^{3+/2+}$ with other complexes are nonadiabatic, as has been observed for some Co(III)–Co(II) cross-reaction systems.[57]

To check on the consistency of the $CoN_4^{3+/2+}$ reactivity, the cross-reaction rate constants for reactions involving $Ru^{II}(NH_3)_4$bpy and selected $Cu^{II}L$ species (Table V) were also analyzed by the Marcus relationship. The resulting k_{11}(Red) values obtained for the $Cu([14]aneS_4)^{2+/+}$ and $Cu([15]aneS_5)^{2+/+}$ systems agree within a factor of 2 of the corresponding values obtained from the cross-reactions with $Co^{II}N_4$ (Table IX). Our inability to observe the reaction between $Cu^{II}(Et_2\text{-}2,3,2\text{-}S_4)$ and $Ru^{II}(NH_3)_4$bpy also agrees qualitatively with the available parameters, which predict that this cross-reaction rate constant should be close to 10^8 M^{-1} s^{-1}. Thus, we conclude that the kinetic results obtained from the $Co^{II}N_4$ reactions are reliable within the limits of experimental error.

Checks of the oxidation kinetics obtained with $Fe^{III}Z_3$ could only be made with the $Cu^{I}(Et_2\text{-}2,3,2\text{-}S_4)$ complex and $Fe^{III}(phen)_3$ and $Fe^{III}(bpy)_3$. However, these reactions did not give consistent results (Table VI).

In an additional attempt to check the consistency of the k_{11}(Ox) values, the cross-reaction rate constants (Table VII) obtained for the reactions of $Cu^{I}([14]aneS_4)$ and $Cu^{I}(Me_2\text{-}2,3,2\text{-}S_4)$ with $Ir^{IV}Cl_6$ were also resolved by using eq 18. The resultant k_{11}(Ox) values calculated from these data are 3.5×10^5 and 1.4×10^8, respectively. These values are, respectively, 10^5 and 10^9 larger than the corresponding values calculated from the kinetic data obtained with $Fe^{III}Z_3$ (Table IX) and strongly suggest that the oxidations with $IrCl_6^{2-}$ are proceeding by an inner-sphere mechanism involving a chloride bridge to an axial site on the copper complexes.[50]

From independent work in this laboratory, it has been established that ClO_4^- and $CF_3SO_3^-$ (designated below as X^-) tend to form adducts with the Cu(II)–polythia ether complexes[55,58]

$$CuL^{2+} + X^- \rightleftharpoons CuLX^+ \tag{26}$$

$$K^\circ_{1X} = \frac{f_{CuLX}}{f_{Cu}f_X}\frac{[CuLX^+]}{[CuL^{2+}][X^-]} \tag{27}$$

where the f terms represent activity coefficients. Although the equilibrium constant for this reaction is relatively small (K°_{1X} = 24 for $Cu^{II}([14]aneS_4)$ with ClO_4^-),[55] the formation of $CuLX^+$ accounts for over half of the total $Cu^{II}L$ in solution in the presence of 0.10 M ClO_4^-.

Since the exact nature of the interaction between the anion and the copper atom in the adduct (including any effect on conformation) is unknown, an examination of the possible influence of the anion upon the Cu(II)/Cu(I) electron-transfer reactivity was undertaken using $Ru^{II}(NH_3)_4$bpy reacting with $Cu^{II}([14]aneS_4)$. A thorough analysis of the kinetic data obtained in four different perchlorate concentrations (Table V) has resulted in the conclusion that CuL^{2+} and $CuLX^+$ exhibit identical electron-transfer properties within the level of experimental error. Although the difference in net charge on these two species results in slight differences in the work terms, the errors engendered by ignoring the existence of $CuLX^+$ appear to be insignificant in 0.10 M $HClO_4$.

On the basis of the foregoing data analyses, conclusions regarding the veracity of the kinetic data may be summarized as follows:

1. The reactions involving $IrCl_6^{2-}$ as an oxidizing agent (and the reaction of $Co^{III}N_4$ with Cu^{I}(aq)) proceed by an inner-sphere mechanism. All other electron-transfer reactions included in this study appear to proceed by outer-sphere mechanisms.

2. The formal potential and self-exchange rate constant available for the $CoN_4^{3+/2+}$ system and the cross-reaction rate constants for the reduction of the $Cu^{II}L$ complexes with this reagent are accurate within the limits of experimental error.

3. The self-exchange rate constant for the $FeZ_3^{3+/2+}$ reagent system may be in error (presumably too large) by a factor of 10 or more. This suggests that the self-exchange rate constants calculated from the kinetics for the oxidation of the $Cu^{I}L$ species with this reagent (i.e., k_{11}(Ox)) may be in error to the same extent but in the opposite direction (presumably too small). The calculated $\bar{k}_{11}$ values should then be in error by the square root of the k_{11}(Ox) error.

4. Since all copper complexes included in this study have been reacted with the same two counterreagents under very similar conditions, the relative similarities or differences observed for the reactivity levels of the various copper–polythia ethers can be assumed to be significant.

Possible Origins of Discrepancies Observed between k_{11}(Red) and k_{11}(Ox) Values. The large differences in the k_{11}(Red) and k_{11}(Ox) values observed for all of the copper–polythia ether systems could, conceivably, arise from errors in the apparent formal potential values for the $Cu^{II}L/Cu^{I}L$ redox couples listed in Table I. As previously noted, these values were obtained from slow-scan cyclic voltammetric measurements. These values may not be representative of the true thermodynamic values if the inner-sphere and solvent reorganization rates accompanying electron transfer at the copper center are kinetically slow relative to the scan rates utilized.

To circumvent the need for preselecting values of E_{11}^f for the various systems studied, eq 18 and 19 can be combined to eliminate E_{11}^f from the Marcus relationship as follows

$$k_{11}(\text{comb}) = \frac{k_{12}k_{13}}{(k_{22}k_{33}K_{32}f_{12}f_{31})^{1/2}W_{12}W_{31}} \tag{28}$$

where

$$K_{32} = K_{12}K_{31} = 10^{(E_{33}^f - E_{22}^f)nF/2.3RT} \tag{29}$$

If one starts with the initial approximation that f_{12} and f_{31} are unity, the initially generated value of k_{11}(comb) may be substituted into eq 18 and 19 to obtain apparent values for K_{12} and K_{31} from which improved estimates of f_{12} and f_{31} can be calculated. In this manner, eq 28 quickly converges to yield values of k_{11}(comb) that closely approximate the values of $\bar{k}_{11}$ (Table IX), the only differences arising from differences in the nonlinear terms as the result of presumed differences in driving potentials. The final value of K_{12} or K_{31} can then be used to calculate an apparent value of E_{11}^f. These apparent E_{11}^f values are tabulated in Table I, where they are compared to the $E_{1/2}$ values estimated from cv measurements.

The E_{11}^f values calculated in the foregoing manner are seen to be widely divergent from the cv-determined $E_{1/2}$ values for these systems. To determine whether the E_{11}^f values calculated from the resolution of eq 28 might be valid, static experiments using controlled-potential electrolysis have been attempted on several of these copper–polythia ether systems.[59] The conclusion reached is that the $E_{1/2}$ values determined from the cyclic voltammetric measurements closely approximate the thermodynamic potentials for these systems. Thus, we conclude that errors in the $E_{1/2}$ values cannot account for the disagreement in the k_{11}(Red) and k_{11}(Ox) values.

Systematic Mechanistic Interpretation. Although the Marcus square root relation (eq 18 and 19) was originally based on the crossing between harmonic potential energy surfaces,[33] this and

(57) (a) Endicott, J. F.; Ramasami, T.; Gaswick, D. C.; Tamilarasan, R.; Heeg, M. J.; Brubaker, G. R.; Pyke, S. C. *J. Am. Chem. Soc.* **1983**, *105*, 5301–5310. (b) Ramasami, T.; Endicott, J. F. *Inorg. Chem.* **1984**, *23*, 3324–3333. (c) Ramasami, T.; Endicott, J. F. *J. Am. Chem. Soc.* **1985**, *107*, 389–396. (d) Endicott, J. F.; Ramasami, T. *J. Phys. Chem.* **1986**, *90*, 3740–3747.

(58) Young, I. R.; Ochrymowycz, L. A.; Rorabacher, D. B. *Inorg. Chem.* **1986**, *25*, 2576–2582.

(59) Rorabacher, D. B.; Bernardo, M. M., work in progress.

very closely related expressions have been used with reasonable success to describe a variety of reactions that involve bond breaking or bond making.[60-64] Consequently, it seems unlikely that large discrepancies between calculated self-exchange rate constants, as determined from oxidation and reduction reactions, can be simply attributed to the anharmonicities that necessarily accompany the change in coordination number encountered upon converting from Cu(II) to Cu(I) (or vice versa). A more systematic consideration of events along the reaction coordinate is required.

As an alternative hypothesis, it is proposed that the reactions involving the reduction of $Cu^{II}L$ and the oxidation of $Cu^{I}L$ (reactions 2a and 3a, respectively) may be proceeding by differnt mechanistic pathways. In consideration of the large conformational differences between $Cu^{II}L$ and $Cu^{I}L$ for most systems, it is conceivable that at least part of the required conformational change may occur sequentially rather than concertedly with the electron-transfer step.[65] Since the sequence of conformational change and electron transfer could occur in either order, the simplest general mechanism that can be devised is a square scheme as represented in eq 30 (corresponding to reaction 2).[66] (For the

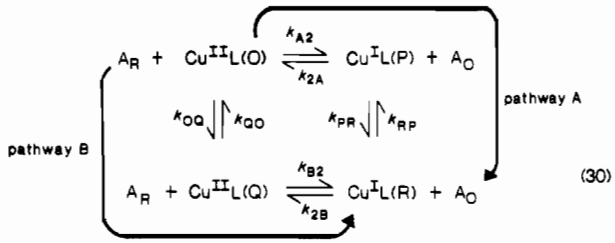

(30)

scheme corresponding to reaction 3, A_R and A_O should be replaced by B_R and B_O and rate constants k_{A2}, k_{2A}, k_{B2}, and k_{2B} should be renumbered as k_{A3}, k_{3A}, k_{B3}, and k_{3B}, respectively.) In this scheme, $Cu^{II}L(O)$ and $Cu^{I}L(R)$ (hereinafter referred to simply as O and R) represent the thermodynamically stable conformers of the oxidant and reductant, respectively, while $Cu^{II}L(Q)$ and $Cu^{I}L(P)$ (hereinafter referred to as Q and P) represent metastable species having coordination geometries more closely approximating the stable geometries of the opposing oxidation states. Thus, by definition, $K_{OQ} = k_{OQ}/k_{QO} < 1 < K_{PR} = k_{PR}/k_{RP}$. Under appropriate conditions, where the steady-state approximation may be applied to species Q and P, rate eq 31 and 32 can be generated

reduction

$$-\frac{d[A_R]}{dt} = \left(\frac{k_{A2}k_{PR}}{k_{2A}[A_O] + k_{PR}} + \frac{k_{B2}k_{OQ}}{k_{B2}[A_R] + k_{QO}}\right)[O][A_R] \quad (31)$$

oxidation

$$-\frac{d[B_O]}{dt} = \left(\frac{k_{3A}k_{RP}}{k_{3A}[B_O] + k_{PR}} + \frac{k_{3B}k_{QO}}{k_{B3}[B_R] + k_{QO}}\right)[R][B_O] \quad (32)$$

to describe the reduction kinetics of $Cu^{II}L$ and the oxidation kinetics of $Cu^{I}L$, respectively. In each equation, the first parenthetical term represents the kinetic contribution of pathway A and the second term represents the contribution of pathway B.

Depending upon the relative magnitude of the two terms in the denominator of each parenthetical term in eq 31 and 32, one may obtain the limiting expressions eq 31a–d and 32a–d. Since all

reduction

pathway A
$$-\frac{d[A_R]}{dt} = k_{A2}[O][A_R] \quad (31a)$$

$$-\frac{d[A_R]}{dt} = K_{A2}k_{PR}\frac{[O][A_R]}{[A_O]} \quad (31b)$$

pathway B
$$-\frac{d[A_R]}{dt} = k_{OQ}[O] \quad (31c)$$

$$-\frac{d[A_R]}{dt} = K_{QO}k_{B2}[O][A_R] \quad (31d)$$

oxidation

pathway A
$$-\frac{d[B_O]}{dt} = k_{RP}[R] \quad (32a)$$

$$-\frac{d[B_O]}{dt} = k_{3A}K_{PR}^{-1}[R][B_O] \quad (32b)$$

pathway B
$$-\frac{d[B_O]}{dt} = k_{3B}[R][B_O] \quad (32c)$$

$$-\frac{d[B_O]}{dt} = K_{B3}^{-1}k_{QO}\frac{[R][B_O]}{[B_R]} \quad (32d)$$

of the reactions included in the current work exhibited second-order kinetics, eq 31c and 32a do not apply. (It is worth noting, however, that several other workers studying Cu(II)/Cu(I) electron-transfer reactions have observed first-order kinetics, which they have interpreted as representing rate-limiting conformational changes.[11,19,68]) Moreover, we have seen no evidence for kinetic inhibition by the products indicating that eq 31b and 32d are also not applicable.

Analysis of the Marcus relationship in terms of the foregoing scheme yields expressions 33–36 for k_{11}(Red) and k_{11}(Ox), re-

pathway A
$$k_{11}(\text{Red}) = k_{AA}K_{PR}^{-1}f_{A2}/f_{12} \quad (33)$$

$$k_{11}(\text{Ox}) = k_{AA}K_{PR}^{-1}f_{3A}/f_{31} \quad (34)$$

pathway B
$$k_{11}(\text{Red}) = k_{BB}K_{OQ}f_{B2}/f_{12} \quad (35)$$

$$k_{11}(\text{Ox}) = k_{BB}K_{OQ}f_{3B}/f_{31} \quad (36)$$

spectively, depending upon the predominant pathway. k_{AA} and k_{BB} are the microscopic self-exchange rate constants defined by symmetric reactions 37 and 38. The terms f_{A2}, f_{B2}, f_{3A}, and f_{3B}

$$*O + P \underset{}{\overset{k_{AA}}{\rightleftharpoons}} *P + O \quad (37)$$

$$*Q + R \underset{}{\overset{k_{BB}}{\rightleftharpoons}} *R + Q \quad (38)$$

represent the nonlinear Marcus terms for reduction of $Cu^{II}L$ by pathways A and B and for oxidation of $Cu^{I}L$ by pathways A and B, respectively. Since the ratios of the nonlinear terms in eq 33–36 should not differ greatly from unity (test data suggest a maximum range of 0.2–5.0), large discrepancies between the calculated values of k_{11}(Red) and k_{11}(Ox) imply that the reduction and oxidation reactions are proceeding by different pathways. (Potential energy surfaces illustrating these pathways are presented in Figure 2.) This is explicable only if the rate constants for a conformational change (specifically k_{OQ} and k_{RP}) are small relative to the pseudo-first-order rate constants for the electron-transfer step ($k_{A2}[A_R]$ and $k_{3B}[B_O]$, respectively) such that reduction occurs

(60) Murdoch, J. R. *J. Am. Chem. Soc.* **1983**, *105*, 2159–2164.
(61) (a) Pellerite, M. S.; Brauman, J. I. *J. Am. Chem. Soc.* **1980**, *102*, 5993–5999. (b) Pellerite, M. S.; Brauman, J. I. *Ibid.* **1983**, *105*, 2672–2680. (c) Pellerite, M. S.; Brauman, J. I. In *Mechanistic Aspects of Inorganic Reactions*: Rorabacher, D. B., Endicott, J. F., Eds.; ACS Symposium Series 198; American Chemical Society: Washington, DC, 1982; pp 81–95.
(62) Wolfe, S.; Mitchell, D. J.; Schlegel, H. B. *J. Am. Chem. Soc.* **1981**, *103*, 7694–7696.
(63) (a) Kumar, K.; Rotzinger, F. P.; Endicott, J. F. *J. Am. Chem. Soc.* **1983**, *105*, 7064–7074. (b) Patel, R. C.; Endicott, J. F. *Ibid.* **1968**, *90*, 6364–6371.
(64) Stanbury, D. M. *Inorg. Chem.* **1984**, *23*, 2914–2916.
(65) This point is analogous to the separate activation of inner-shell and solvent vibrational modes when these have very different relaxation times. The mode with the longer relaxation time will tend to appear as a prequilibrium term in the overall rate expression: Newton, M. D.; Sutin, N. *Annu. Rev. Phys. Chem.* **1984**, *35*, 437–480.
(66) Laviron, E.; Roullier, L. *J. Electroanal. Chem. Interfacial Electrochem.* **1985**, *186*, 1–15.
(67) Allan, A. E.; Lappin, A. G.; Laranjeira, M. C. M. *Inorg. Chem.* **1984**, *23*, 477–482.
(68) (a) Rosen, P.; Pecht, I. *Biochemistry* **1976**, *15*, 775–786. (b) Wilson, M. T.; Greenwood, C.; Brunori, M.; Antonini, E. *Biochem. J.* **1975**, *145*, 449–457.

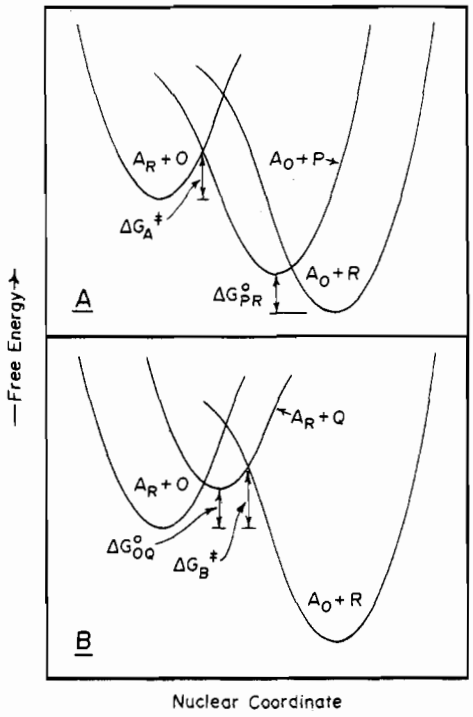

Figure 2. Qualitative potential energy surfaces illustrating the possible contributions of conformational isomerizations to electron-transfer reactions involving $CuL^{2+/+}$ couples. In pathway A (top), electron transfer produces a metastable conformational isomer (P) of the product species; in pathway B (bottom), a conformational preequilibrium precedes electron transfer. Terms are referenced to eq 30 as defined in the text. The two-dimensional free-energy surfaces are drawn with distortions to reflect the very large amplitude nuclear displacements that accompany the net reaction.

primarily via pathway A and oxidation primarily via pathway B; i.e., k_{11}(Red) and k_{11}(Ox) are represented by eq 33 and 36, respectively.

Independent Evidence for the Square Scheme. In studying both the oxidation and reduction kinetics of a substituted polypyridyl complex of copper ion, Lappin and co-workers[67] concluded that the mechanism for the reduction reaction involved two conformers of the Cu(II) complex, corresponding to our pathway B in the proposed square scheme. Moreover, these workers proposed that the metastable Cu(II) intermediate was a tetrahedral species closely resembling the stable Cu(I) complex. Similar interpretations have been reported for this or closely related reactions by Sykes and co-workers[30] and by Davies.[31] For similar electron-transfer reactions involving blue electron carriers, observations of both second- and first-order kinetic behaviors have, in fact, been directly observed in the case of the reduction of rusticyanin[19] and the oxidation of azurin.[11,68] Both of these observations have been attributed to conformational changes occurring at the copper site prior to the electron-transfer step (i.e., corresponding to our proposed pathways B and A, respectively). In the case of the reduction of rusticyanin, the use of a very strong reducing agent (chromium(II)) resulted in a second-order rate that exceeded the limiting first-order behavior.[19] Within the context of the square scheme, this could be explained in terms of a switch from pathway B to pathway A as the driving force becomes very large such that $k_{A2}[A_R]$ (eq 31a) exceeds k_{OQ} (eq 31c), which is constant. It is also pertinent that, for both rusticyanin and azurin, independent spectral evidence for the existence of two stable or metastable conformers of the copper site has been obtained.[19,69]

In recent electrochemical studies conducted in this laboratory,[70] direct evidence for two distinct electron-transfer pathways has

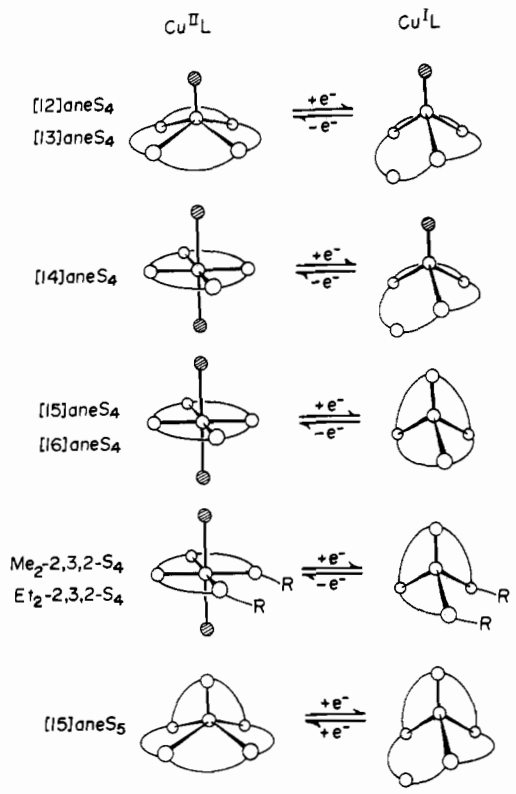

Figure 3. Schematic representations of the changes taking place in the inner-coordination sphere of the copper atom upon oxidation or reduction as inferred from crystallographic structures and molecular models for the copper–polythia ether complexes included in this work. All structures shown are intended to represent the stable forms of $Cu^{II}L$ and $Cu^{I}L$ (i.e., species O and R, respectively). Unshaded atoms represent the central copper atoms and the sulfur donor atoms while the shaded atoms represent coordinated solvent molecules or anions (i.e., H_2O, ClO_4^-, or $CF_3SO_3^-$).

been obtained in the case of $Cu([14]aneS_4)^{2+/+}$ and $Cu(Et_2\text{-}2,3,2\text{-}S_4)^{2+/+}$. By contrast, $Cu([15]aneS_5)^{2+/+}$ appears to exhibit the presence of only a single reversible redox couple over a wide range of conditions.

The differing kinetic behavior noted for the various copper–polythia ether complexes may be correlated to the apparent structural changes that accompany electron transfer in these systems. Extrapolation of crystallographic structural data to solution conditions suggests that the following structural changes accompany the reduction of $Cu^{II}L$ complexes, as illustrated schematically in Figure 3:

(1) For $Cu^{II}([14]aneS_4)$, one planar Cu–S bond and one axial $Cu\text{–}OH_2$ bond are ruptured with the remaining three Cu–S bonds and one $Cu\text{–}OH_2$ bond forming a tetrahedral coordination environment.[39]

(2) By analogy to the foregoing system, it is inferred for $Cu^{II}([12]aneS_4)$ and $Cu^{II}([13]aneS_4)$ that one Cu–S bond is ruptured with the three remaining Cu–S bonds and the only existing $Cu\text{–}OH_2$ bond forming a tetrahedron.[38]

(3) For $Cu^{II}([15]aneS_4)$ and $Cu^{II}([16]aneS_4)$, structural models indicate that a tetrahedral environment can be achieved by the four Cu–S bonds, suggesting that only the two axial $Cu\text{–}OH_2$ bonds need be broken.[38] These latter bonds are apparently very weak.

(4) For $Cu^{II}(Et_2\text{-}2,3,2\text{-}S_4)$ and $Cu^{II}(Me_2\text{-}2,3,2\text{-}S_4)$, molecular models suggest that the four Cu–S bonds can adapt to a tetrahedral coordination sphere upon rupture of the two axial $Cu\text{–}OH_2$ bonds.[39] However, in the absence of a macrocyclic structure to stabilize the $Cu^{II}L$ complex, it is believed that fewer than four S atoms are coordinated to Cu(II) on a time-averaged basis. This may account for the difference in observed behavior for the open-chain complexes as compared to the $Cu([16]aneS_4)^{2+/+}$ and $Cu([15]aneS_4)^{2+/+}$ systems.

(69) Szabo, A. G.; Stepanik, T. M.; Wayner, D. M.; Young, N. M. *Biophys. J.* **1983**, *41*, 233–244.
(70) Bernardo, M. M.; Schroeder, R. R.; Rorabacher, D. B., submitted for publication.

(5) For $Cu^{II}([15]aneS_5)$, one "planar" Cu-S bond is ruptured with the four remaining Cu-S bonds requiring little rearrangement to achieve a stable tetrahedral coordination sphere.[40]

We conclude that (i) as the coordinated donor atoms undergoing bond rupture are limited to weakly held axial donor atoms and (ii) inner-sphere rearrangement is minimized, the ratio of k_{11}(Red) to k_{11}(Ox) more closely approximates unity in the current series of copper complexes. These conclusions will be examined further in future studies.

Acknowledgment. This work was supported, in part, by the National Institute of General Medical Sciences under Grant GM-20424 (to L.A.O. and D.B.R.)

Registry No. $Cu([12]aneS_4)^{2+}$, 57673-84-4; $Cu([13]aneS_4)^{2+}$, 57673-85-5; $Cu([14]aneS_4)^{2+}$, 57673-86-6; $Cu([15]aneS_4)^{2+}$, 57673-87-7; $Cu([16]aneS_4)^{2+}$, 57673-88-8; $Cu([15]aneS_5)^{2+}$, 60165-93-7; $Cu(Me_2\text{-}2,3,2\text{-}S_4)^{2+}$, 60165-82-4; $Cu(Et_2\text{-}2,3,2\text{-}S_4)^{2+}$, 57673-90-2; $Cu([12]aneS_4)^{+}$, 87464-60-6; $Cu([13]aneS_4)^{+}$, 87464-61-7; $Cu([14]aneS_4)^{+}$, 93645-98-8; $Cu([15]aneS_4)^{+}$, 87464-64-0; $Cu([16]aneS_4)^{+}$, 59918-91-1; $Cu([15]aneS_5)^{+}$, 87464-65-1; $Cu(Me_2\text{-}2,3,2\text{-}S_4)^{+}$, 87464-68-4; $Cu(Et_2\text{-}2,3,2\text{-}S_4)^{+}$, 87464-69-5; $Fe(4,7\text{-}Me_2phen)_3^{3+}$, 17378-76-6; $[Co(Me_4[14]tetraeneN_4)(H_2O)_2]^{2+}$, 38337-82-5; $Ru(NH_3)_4bpy^{2+}$, 54194-87-5; $Fe(phen)_3^{3+}$, 13479-49-7; $Fe(bpy)_3^{3+}$, 18661-69-3; $IrCl_6^{2-}$, 16918-91-5.

Contribution from the Department of Physics, The Pennsylvania State University, University Park, Pennsylvania 16802, and Departments of Chemistry, University of Notre Dame, Notre Dame, Indiana 46556, and University of Southern California, Los Angeles, California 90089-1062

Spin Coupling in Admixed Intermediate-Spin Iron(III) Porphyrin Dimers: Crystal Structure, Mössbauer, and Susceptibility Study of $Fe(TPP)(B_{11}CH_{12})\cdot C_7H_8$

Govind P. Gupta,[†‡] George Lang,*[†] Young Ja Lee,[§] W. Robert Scheidt,*[§] Kenneth Shelly,[∥] and Christopher A. Reed*[∥]

Received March 3, 1987

Susceptibility measurements on $Fe(TPP)(B_{11}CH_{12})\cdot C_7H_8$ (TPP = tetraphenylporphyrinate) in an external field of 0.2 T show that its magnetic moment varies from 2.0 to 4.2 μ_B over the temperature range 6-300 K. The data were analyzed with "Maltempo model" spins antiferromagnetically coupled within dimers. Face-to-face pairing of molecules is seen in the crystal structure. The analysis shows that the ground-state quartet $S = {}^3/_2$ (92%) is mixed with the nearby sextet $S = {}^5/_2$ (8%) through spin-orbit coupling with an unusually small coupling constant, $\xi = 150$ cm^{-1}. The exchange interaction within the dimer is estimated to be $\sim +(3.0$ cm$^{-1})\vec{S}_1\cdot\vec{S}_2$. Mössbauer spectra were recorded at temperatures varying from 4.2 to 128 K in fields 0-6 T. The chemical shift $\delta = 0.33$ mm/s (Fe) and quadrupole splitting $\Delta E_Q = 4.12$ mm/s are temperature-independent and typical of ferric ions in the admixed intermediate-spin state. Mössbauer analysis confirms the exchange interaction between the two spin systems in the dimer. The analysis also provides the rather low contact hyperfine field $P\kappa/g_N\beta_N = 8.7$ T/unit spin. The spectra imply intermediate relaxation rates even in fields of 6 T at 4.2 K, the rate increasing with increasing T and decreasing H. All Mössbauer and susceptibility data were fitted with a common parameter set; only the relaxation parameter was varied from one spectrum to another. The $[Fe(TPP)(B_{11}CH_{12})]\cdot C_7H_8$ complex is found to be five-coordinate with the carborane anion as the axial ligand with an open Fe-H-B bridge bond. The Fe-H distance is 1.82 (4) Å, and the Fe-H-B angle is 151 (3)°. The complex also has very short Fe-N bonds: the average distance is 1.961 (5) Å. The complex also exhibits an interaction between pairs of molecules suggestive of a significant π-π interaction. The separation between mean porphinato planes is 3.83 Å. Crystal data for $[Fe(TPP)(B_{11}CH_{12})]\cdot C_7H_8$: triclinic, $a = 13.660$ (2) Å, $b = 14.656$ (3) Å, $c = 13.142$ (2) Å, $\alpha = 94.85$ (1)°, $\beta = 109.63$ (1)°, $\gamma = 75.81$ (1)°, $Z = 2$, space group $P\bar{1}$, 7446 unique observed data, $R_1 = 0.079$, $R_2 = 0.092$, all observations at 293 K.

Although intermediate-spin iron(III) prophyrin complexes with apparent admixture ($S = {}^3/_2, {}^5/_2$) have been known[1] for about a decade, quantitative descriptions of their electronic structures in terms of the quantum-mechanical admixture theory of Maltempo[2] have been only partially successful.[3,4] Qualitatively, it is known that intermediate-spin states arise from highly tetragonal ligand fields, typically in five-coordinate complexes of the type Fe(Porph)Y where Y is a weak-field ligand (ClO_4^-, SbF_6^-, etc.). Room-temperature magnetic moments in the range 4.0-5.2 μ_B and $g_\perp$ values in the range 4.2-4.9 suggest widely varying degrees of admixture of $S = {}^5/_2$ character into the $S = {}^3/_2$ state although one recent interpretation dispenses with the admixture concept in favor of an empirically assigned Zeeman term g anisotropy.[5] We have accumulated variable-temperature and variable-field magnetic susceptibility and Mössbauer data on such complexes in recent years but have found a satisfactory congruence of theory and experiment only for $[Fe(OEP)(3\text{-}Cl\text{-}py)][ClO_4]$[6] and for the hexafluoroantimonate complex $Fe(TPP)(FSbF_5)\cdot C_6H_5F$.[7] The treatment in the latter case involved the use of the Maltempo model with 98% $S = {}^3/_2$ contribution to the ground state and a very small spin-orbit coupling constant ζ of 79 cm^{-1}. In addition it was necessary to postulate a nonspecific, short-range antiferromagnetic interaction that at low temperatures effectively couples all the spins of the crystal. In the present paper we find that a satisfactory treatment of Mössbauer and susceptibility data for the related carboranyl complex $Fe(TPP)(B_{11}CH_{12})\cdot C_7H_8$ can be obtained by using a Maltempo model along with pairwise intermolecular antiferromagnetic coupling. The face-to-face pairing of the five-coordinate hemes that is seen in the X-ray crystallo-

[†] The Pennsylvania State University.

[‡] On leave from the Physics Department, Lucknow University, Lucknow, India.

[§] University of Notre Dame.

[∥] University of Southern California.

(1) Dolphin, D. H.; Sams, J. R.; Tsin, T. B. *Inorg. Chem.* **1977**, *16*, 711. Masuda, H.; Taga, T.; Osaki, K.; Sugimoto, H.; Yoshida, Z.; Ogoshi, H. *Inorg. Chem.* **1980**, *19*, 950. Reed, C. A.; Mashiko, T.; Bentley, S. P.; Kastner, M. E.; Scheidt, W. R.; Spartalian, K.; Lang, G. *J. Am. Chem. Soc.* **1979**, *101*, 2948.
(2) Maltempo, M. M.; Moss, T. H. *Q. Rev. Biophys.* **1976**, *9*, 181.
(3) Spartalian, K.; Lang, G.; Reed, C. A. *J. Chem. Phys.* **1979**, *71*, 1832.
(4) Mitra, S.; Marathe, V. R.; Birdy, R. *Chem. Phys. Lett.* **1983**, *96*, 103.
(5) Ichimori, K.; Ohya-Nishiguchi, H.; Hirota, N.; Masuda, H.; Ogoshi, H. *Chem. Phys. Lett.* **1986**, *124*, 401.
(6) Gupta, G. P.; Lang, G.; Scheidt, W. R.; Geiger, D. K.; Reed, C. A. *J. Chem. Phys.* **1986**, *85*, 5212.
(7) Gupta, G. P.; Lang, G.; Reed, C. A.; Shelly, K.; Scheidt, W. R. *J. Chem. Phys.* **1987**, *86*, 5288.
(8) Gupta, G. P.; Lang, G.; Scheidt, W. R.; Geiger, D. K.; Reed, C. A. *J. Chem. Phys.* **1985**, *83*, 5945.

0020-1669/87/1326-3022$01.50/0 © 1987 American Chemical Society